Pergamon

*Int. J. Solids Structures* Vol. 33, No. 19, pp. 2817–2840, 1996

0020–7683/96 $15.00 + .00

0020–7683(95)00148–4

# SCATTERING OF ELASTIC WAVES BY A RIGID CYLINDRICAL INCLUSION PARTIALLY DEBONDED FROM ITS SURROUNDING MATRIX—II. P AND SV CASES

YUE-SHENG WANG and DUO WANG†

Department of Astronautics and Mechanics, P.O. Box 344, Harbin Institute of Technology, Harbin 150001, People's Republic of China

(*Received* 18 *April* 1994; *in revised form* 23 *June* 1995)

**Abstract**—This is Part II of a two-part paper which analyses the scattering of elastic waves by a rigid cylindrical inclusion partially debonded from its surrounding matrix. The scattering of SH waves was solved in Part I by the use of the wave function expansion method and singular integral equation technique. Here, in Part II, we consider the scattering of P and SV waves by using a similar approach. As in Part I, the debonds are modeled as interface cracks with noncontacting faces. Then the problems are reduced to a set of singular integral equations of the second type in terms of the dislocation density functions, which demonstrates the oscillatory behavior of the stresses near the crack tips. By representing the dislocation density functions with Jacobi polynomials, these equations are solved numerically. Two limiting situations are considered: the long wavelength limit with arbitrary debond sizes and the small debond limit with $K_{T0}r_0 = O(1)$ (where $K_{T0}$ is the shear wavenumber and $r_0$ the inclusion radius). The general solution simplifies in these two limiting cases and results, similar to those for SH case, are obtained. Finally, the numerical results for the dynamic stress intensity factors, rigid body motion of the inclusion, and scattering cross-sections are presented for both P and SV cases, and the low frequency resonance phenomenon, as in SH case, is explored.


## 1. INTRODUCTION

In Part I of this two-part paper (Wang and Wang, 1996) the problem of SH wave scattering by a rigid cylindrical inclusion partially debonded from matrix was discussed. The problem resulted in a set of singular integral equations of the first kind with the dislocation density functions being unknowns. A quadrature method was used to solved these integral equations. The numerical results for the near and far fields were presented, and the explicit solutions for the long wavelength limit and the small debond limit were obtained. In Part II, a similar approach will be used to deal with the scattering of P and SV waves.

Figure 1 shows a rigid cylindrical inclusion, with radius $r_0$ and mass density $\rho_1$, partially debonded from its surrounding matrix. An incident P or SV wave propagates in the $\theta_0$-direction. In Fig. 1, the cylindrical coordinate $(r, \theta, z)$ is used and the $\theta$ coordinates of the

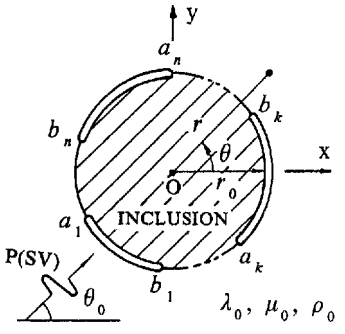


Fig. 1. A P- or SV-wave incident on a rigid cylindrical inclusion partially debonded from elastic matrix.

† Present address: Institute of Engineering Mechanics, North Jiaotong University, Beijing 100044, People's Republic of China.

$k$th crack tips are assumed to be $a_k$ and $b_k$ ($k = 1$–$n$). Obviously, the problem considered here is the plane-strain problem. If we treat the debonds as interface cracks with non-contacting faces, the stresses near the crack tips will have oscillatory inverse square-root behavior, which makes the problem very difficult to deal with. The singular integral equation method has been proved to be successful in solving such a problem and has been used widely in dealing with the elastic wave scattering by a flat interface crack between two bonded half-space (Srivastava *et al.*, 1978; Yang and Bogy, 1985). In the present paper, this method will be applied to analyse the dynamic problem of arc-shaped interface cracks between a rigid cylindrical inclusion and elastic matrix.

The scattering of P waves from a partially debonded elastic cylindrical inclusion was also attacked by Coussy (1983) and Yang and Norris (1992). Coussy (1983) gave the far-field solution for the long wavelength limit. Yang and Norris (1992) presented numerical results of near and far fields for arbitrary frequencies. But they limited their analysis to the special material combinations for which the oscillation parameter vanishes.

## 2. FORMULATION OF THE PROBLEM

For the present dynamic plane-strain problem, the displacement components in the $r$- and $\theta$-direction denoted by $u_0$ and $v_0$ can be expressed in terms of two wave potentials $\varphi_0$ and $\psi_0$, they may be written as (Pao and Mow, 1973):

$$\begin{cases} u_0 = \dfrac{\partial \varphi_0}{\partial r} + \dfrac{1}{r}\dfrac{\partial \psi_0}{\partial \theta}, \\ v_0 = \dfrac{1}{r}\dfrac{\partial \varphi_0}{\partial \theta} - \dfrac{\partial \psi_0}{\partial r}. \end{cases} \tag{1}$$

Then the stress–potential relations for the two stress components $\sigma_{r0}$ and $\tau_{r\theta 0}$ needed here become

$$\begin{cases} \sigma_{r0} = \lambda_0 \nabla^2 \varphi_0 + 2\mu_0 \dfrac{\partial}{\partial r}\left(\dfrac{\partial \varphi_0}{\partial r} + \dfrac{1}{r}\dfrac{\partial \psi_0}{\partial \theta}\right), \\ \tau_{r\theta 0} = \mu_0 \left(\dfrac{2}{r}\dfrac{\partial^2 \varphi_0}{\partial r \partial \theta} - \dfrac{2}{r^2}\dfrac{\partial \varphi_0}{\partial \theta} - \dfrac{\partial^2 \psi_0}{\partial r^2} + \dfrac{1}{r}\dfrac{\partial \psi_0}{\partial r} + \dfrac{1}{r^2}\dfrac{\partial^2 \psi_0}{\partial \theta^2}\right), \end{cases} \tag{2}$$

where

$$\nabla^2 = \frac{\partial^2}{\partial r^2} + \frac{1}{r}\frac{\partial}{\partial r} + \frac{1}{r^2}\frac{\partial^2}{\partial \theta^2}.$$

In terms of these potentials, the equations of motion reduce to

$$\nabla^2 \varphi_0 + K_{L0}^2 \varphi_0 = 0, \quad \nabla^2 \psi_0 + K_{T0}^2 \psi_0 = 0, \tag{3}$$

where $K_{L0} = \omega / C_{L0}$ and $K_{T0} = \omega / C_{T0}$ are longitudinal and shear wavenumbers respectively, $C_{L0} = \sqrt{(\lambda_0 + 2\mu_0)/\rho_0}$ and $C_{T0} = \sqrt{\mu_0/\rho_0}$ are wave velocities, and $\lambda_0$, $\mu_0$, $\rho_0$ denote the Lamés constants and mass density of the elastic matrix.

Without loss of generality, let us consider the incident wave with the form

$$\varphi_0^{(i)}(r, \theta) = A\, e^{iK_{L0} r \cos(\theta - \theta_0)}, \quad \psi_0^{(i)}(r, \theta) = 0, \tag{4}$$

for the incident P wave, or

$$\varphi_0^{(i)}(r,\theta)=0,\quad \psi_0^{(i)}(r,\theta)=A\,\mathrm{e}^{\mathrm{i}K_{\mathrm{T}0}r\cos(\theta-\theta_0)},\tag{5}$$

for the incident SV wave, where $A$ in above two equations is amplitude.

The following analysis will focus on the incident P wave. The results for the incident SV wave can be obtained analogously.

Because of linearity, the principle of superposition can be used to decompose the total potentials in the elastic matrix as

$$\begin{cases}\varphi_0(r,\theta)=\varphi_0^{(i)}(r,\theta)+\varphi_0^{(0)}(r,\theta)+\varphi_0^{(1)}(r,\theta),\\ \psi_0(r,\theta)=\psi_0^{(0)}(r,\theta)+\psi_0^{(1)}(r,\theta),\end{cases}\tag{6}$$

where $\varphi_0^{(0)}$ and $\psi_0^{(0)}$ are potentials for the scattered fields that would be present if the inclusion were perfectly bonded (Pao and Mow, 1973), while $\varphi_0^{(1)}$ and $\psi_0^{(1)}$ are those for the additional scattered fields generated by the debonds which, by the use of the wave function expansion method (Pao and Mow, 1973), can be written as

$$\begin{cases}\varphi_0^{(1)}(r,\theta)=\displaystyle\sum_{m=-\infty}^{\infty}A_mH_m^{(1)}(K_{\mathrm{L}0}r)\,\mathrm{e}^{-\mathrm{i}m\theta},\\ \psi_0^{(1)}(r,\theta)=\displaystyle\sum_{m=-\infty}^{\infty}B_mH_m^{(1)}(K_{\mathrm{T}0}r)\,\mathrm{e}^{-\mathrm{i}m\theta},\end{cases}\tag{7}$$

with $A_m$ and $B_m$ unknown. Then from eqns (1) and (2) we have

$$\begin{cases}u_0^{(1)}(r,\theta)=\dfrac{1}{r}\displaystyle\sum_{m=-\infty}^{\infty}[A_mK_{\mathrm{L}0}rH_m^{(1)\prime}(K_{\mathrm{L}0}r)-\mathrm{i}B_mmH_m^{(1)}(K_{\mathrm{T}0}r)]\,\mathrm{e}^{-\mathrm{i}m\theta}\\ v_0^{(1)}(r,\theta)=\dfrac{1}{r}\displaystyle\sum_{m=-\infty}^{\infty}[-\mathrm{i}A_mmH_m^{(1)}(K_{\mathrm{L}0}r)-B_mK_{\mathrm{T}0}rH_m^{(1)\prime}(K_{\mathrm{T}0}r)]\,\mathrm{e}^{-\mathrm{i}m\theta},\end{cases}\tag{8}$$

and

$$\begin{cases}\sigma_{r0}^{(1)}(r,\theta)=\dfrac{\mu_0}{r^2}\displaystyle\sum_{m=-\infty}^{\infty}[A_mT_{11}^{(m)}(K_{\mathrm{L}0}r)+B_mT_{12}^{(m)}(K_{\mathrm{T}0}r)]\,\mathrm{e}^{-\mathrm{i}m\theta}\\ \tau_{r\theta0}^{(1)}(r,\theta)=\dfrac{\mu_0}{r^2}\displaystyle\sum_{m=-\infty}^{\infty}[A_mT_{21}^{(m)}(K_{\mathrm{L}0}r)+B_mT_{22}^{(m)}(K_{\mathrm{T}0}r)]\,\mathrm{e}^{-\mathrm{i}m\theta},\end{cases}\tag{9}$$

where

$$\begin{cases}T_{11}^{(m)}(z)=-T_{22}^{(m)}(z)=(2m^2-K_{\mathrm{T}0}^2r^2)H_m^{(1)}(z)-2zH_m^{(1)\prime}(z),\\ T_{12}^{(m)}(z)=T_{21}^{(m)}(z)=2\mathrm{i}m[H_m^{(1)}(z)-zH_m^{(1)\prime}(z)].\end{cases}\tag{10}$$

For a movable inclusion, we should also consider the motion of the inclusion. Under the action of P or SV waves, the inclusion will translate and rotate as a rigid body with its harmonic in-plane motion $U\mathrm{e}^{-\mathrm{i}\omega t}$, $V\mathrm{e}^{-\mathrm{i}\omega t}$ and $\Theta\mathrm{e}^{-\mathrm{i}\omega t}$ where $U$ and $V$ denote the amplitude of the rigid body translations in $x$- and $y$-directions, respectively, and $\Theta$ the amplitude of the rigid body rotation. Decompose $U$, $V$ and $\Theta$ as

$$U=U^{(0)}+U^{(1)},\quad V=V^{(0)}+V^{(1)},\quad \Theta=\Theta^{(0)}+\Theta^{(1)},\tag{11}$$

where $U^{(0)}$, $V^{(0)}$, and $\Theta^{(0)}$ are generated by a perfectly bonded inclusion (Pao and Mow, 1973), while $U^{(1)}$, $V^{(1)}$, and $\Theta^{(1)}$ are due to debonding, which are governed by the following kinetic equations

$$\begin{cases} -\pi\omega^2 r_0^2 \rho_1 U^{(1)} = \displaystyle\int_{-\pi}^{\pi} r_0[\sigma_{r0}^{(1)}(r_0,\theta)\cos\theta - \tau_{r\theta 0}^{(1)}(r_0,\theta)\sin\theta]\,\mathrm{d}\theta \\ -\pi\omega^2 r_0^2 \rho_1 V^{(1)} = \displaystyle\int_{-\pi}^{\pi} r_0[\sigma_{r0}^{(1)}(r_0,\theta)\sin\theta + \tau_{r\theta 0}^{(1)}(r_0,\theta)\cos\theta]\,\mathrm{d}\theta \\ -\dfrac{\pi}{2}\omega^2 r_0^4 \rho_1 \Theta^{(1)} = \displaystyle\int_{-\pi}^{\pi} r_0^2 \tau_{r\theta 0}^{(1)}(r_0,\theta)\,\mathrm{d}\theta. \end{cases} \tag{12}$$

Substituting eqn (9) into eqn (12) yields

$$\begin{cases} U^{(1)} = \dfrac{\rho}{r_0}\{[A_1 - A_{-1}]H_1^{(1)}(K_{\mathrm{L}0}r_0) - \mathrm{i}[B_1 + B_{-1}]H_1^{(1)}(K_{\mathrm{T}0}r_0)\} \\ V^{(1)} = \dfrac{\rho}{r_0}\{-\mathrm{i}[A_1 + A_{-1}]H_1^{(1)}(K_{\mathrm{L}0}r_0) - [B_1 - B_{-1}]H_1^{(1)}(K_{\mathrm{T}0}r_0)\} \\ \Theta^{(1)} = -\dfrac{4\rho}{r_0^2}\left[H_0^{(1)}(K_{\mathrm{T}0}r_0) + \dfrac{2}{K_{\mathrm{T}0}r_0}H_0^{(1)'}(K_{\mathrm{T}0}r_0)\right]B_0, \end{cases} \tag{13}$$

with $\rho = \rho_0/\rho_1$ and $A_{\pm 1}$, $B_{\pm 1}$, $B_0$ unknown.

The interface conditions of the problem may be expressed as

$$u_0^{(1)}(r_0,\theta) = \Delta u(\theta), \quad v_0^{(1)}(r_0,\theta) = \Delta v(\theta), \tag{14}$$

for a fixed rigid inclusion, or

$$\begin{cases} u_0^{(1)}(r_0,\theta) - U^{(1)}\cos\theta - V^{(1)}\sin\theta = \Delta u(\theta) \\ v_0^{(1)}(r_0,\theta) + U^{(1)}\sin\theta - U^{(1)}\cos\theta - r_0\Theta^{(1)} = \Delta v(\theta), \end{cases} \tag{15}$$

for a movable rigid inclusion.

In eqns (14) and (15) $\Delta u$ and $\Delta v$ are the discontinuities of displacements across the interface, which can be expressed as:

$$\Delta u(\theta) = \begin{cases} 0 & \theta \notin (a_k, b_k) \\ \Delta u_k(\theta) & \theta \in (a_k, b_k) \end{cases}, \quad \Delta v(\theta) = \begin{cases} 0 & \theta \notin (a_k, b_k) \\ \Delta v_k(\theta) & \theta \in (a_k, b_k) \end{cases} \tag{16}$$

with $\Delta u_k$ and $\Delta v_k$ denoting the CODs of the $k$th crack.

The total tractions vanish on the crack faces, which implies

$$\sigma_{r0}^{(1)}(r_0,\theta) = -\sigma(\theta); \quad \tau_{r\theta 0}^{(1)}(r_0,\theta) = -\tau(\theta), \quad \theta \in (a_k, b_k) \tag{17}$$

where we have denoted $\sigma(\theta) = \sigma_{r0}^{(i)}(r_0,\theta) + \sigma_{r0}^{(0)}(r_0,\theta)$ and $\tau(\theta) = \tau_{r\theta 0}^{(i)}(r_0,\theta) + \tau_{r\theta 0}^{(0)}(r_0,\theta)$.

Up to now, the problem has been reduced to determination of unknown coefficiences $A_m$ and $B_m$ by the mixed boundary conditions (14)–(17).

## 3. DERIVATION OF THE SINGULAR INTEGRAL EQUATIONS

Expanding $\Delta u(\theta)$ and $\Delta v(\theta)$ in series of $\mathrm{e}^{-\mathrm{i}m\theta}$

$$\Delta u(\theta) = \sum_{m=-\infty}^{\infty} \Delta\bar{u}_m \mathrm{e}^{-\mathrm{i}m\theta}, \quad \Delta v(\theta) = \sum_{m=-\infty}^{\infty} \Delta\bar{v}_m \mathrm{e}^{-\mathrm{i}m\theta}, \tag{18}$$

where

$$\Delta\bar{u}_m = \frac{1}{2\pi}\sum_{l=1}^{n}\int_{a_l}^{b_l}\Delta u_l(\zeta)\,e^{im\zeta}\,d\zeta, \quad \Delta\bar{v}_m = \frac{1}{2\pi}\sum_{l=1}^{n}\int_{a_l}^{b_l}\Delta v_l(\zeta)\,e^{im\zeta}\,d\zeta, \tag{19}$$

we have, from eqns (8) and (14)

$$\begin{cases} A_m = r_0 D_m^{-1}[-K_{T0}r_0 H_m^{(1)'}(K_{T0}r_0)\Delta\bar{u}_m + imH_m^{(1)}(K_{T0}r_0)\Delta\bar{v}_m] \\ B_m = r_0 D_m^{-1}[imH_m^{(1)}(K_{L0}r_0)\Delta\bar{u}_m + K_{L0}r_0 H_m^{(1)'}(K_{L0}r_0)\Delta\bar{v}_m] \end{cases} \tag{20}$$

with

$$D_m = m^2 H_m^{(1)}(K_{L0}r_0)H_m^{(1)}(K_{T0}r_0) - K_{L0}K_{T0}r_0^2 H_m^{(1)'}(K_{L0}r_0)H_m^{(1)'}(K_{T0}r_0), \tag{21}$$

for a fixed rigid inclusion.

From eqns (8), (13) and (15) we can see that for a movable rigid inclusion $A_0$, $A_m$ and $B_m$ for $m \neq \pm 1$ are the same as eqn (20), but that $B_0$, $A_{\pm 1}$ and $B_{\pm 1}$ are different. They are

$$\begin{cases} B_0 = r_0\left\{K_{T0}r_0 H_0^{(1)'}(K_{T0}r_0) - 4\rho\left[H_0^{(1)}(K_{T0}r_0) + \dfrac{2}{K_{T0}r_0}H_0^{(1)'}(K_{T0}r_0)\right]\right\}^{-1}\Delta\bar{v}_0 \\ A_{\pm 1} = r_0 D_1^{-1}\{[\mp K_{T0}r_0 H_0^{(1)}(K_{T0}r_0) + (1+\rho)H_1^{(1)}(K_{T0}r_0)]\Delta\bar{u}_{\pm 1} \pm i(1-\rho)H_1^{(1)}(K_{T0}r_0)\Delta\bar{v}_{\pm 1}\} \\ B_{\pm 1} = r_0 D_1^{-1}\{\pm i(1-\rho)H_0^{(1)}(K_{L0}r_0)\Delta\bar{u}_{\pm 1} \pm [K_{L0}r_0 H_1^{(1)}(K_{T0}r_0) \mp (1+\rho)H_1^{(1)}(K_{L0}r_0)]\Delta\bar{v}_{\pm 1}\} \end{cases} \tag{22}$$

where

$$\begin{aligned} D_1 = {} & (1+\rho)K_{L0}r_0 H_0^{(1)}(K_{L0}r_0)H_1^{(1)}(K_{T0}r_0) + (1+\rho)K_{T0}r_0 H_0^{(1)}(K_{T0}r_0)H_1^{(1)}(K_{L0}r_0) \\ & - K_{L0}K_{T0}r_0^2 H_0^{(1)}(K_{L0}r_0)H_0^{(1)}(K_{T0}r_0) - 4\rho H_1^{(1)}(K_{L0}r_0)H_1^{(1)}(K_{T0}r_0). \end{aligned} \tag{23}$$

It can be shown that when $\rho = 0$, that is, the inclusion is an infinitely dense inclusion, the rigid body motion vanishes. This is the same as fixing the inclusion stationary in space. Thus, the results for a fixed inclusion can be obtained from those for a movable inclusion by setting $\rho = 0$ and we will focus our attention on the case of a movable inclusion in the following analysis.

Substituting eqn (9) into eqn (17) and considering eqns (20) and (22), we obtain

$$\begin{cases} \mu_0 \sum_{m=-\infty}^{\infty}[N_m^{(11)}\Delta\bar{u}_m + N_m^{(12)}\Delta\bar{v}_m]\,e^{-im\theta} = -\sigma(\theta) \\ \mu_0 \sum_{m=-\infty}^{\infty}[N_m^{(21)}\Delta\bar{u}_m + N_m^{(22)}\Delta\bar{v}_m]\,e^{-im\theta} = -\tau(\theta) \end{cases} \qquad \theta \in (a_k, b_k) \tag{24}$$

where $N_m^{(ij)}$ is given in the Appendix.

The continuity of displacements across the interface on the bonding regions implies

$$\sum_{m=-\infty}^{\infty}\Delta\bar{u}_m\,e^{-im\theta} = 0; \quad \sum_{m=-\infty}^{\infty}\Delta\bar{v}_m\,e^{-im\theta} = 0, \quad \theta \notin (a_k, b_k). \tag{25}$$

Equations (24) and (25) are dual series equations of the problem. We will solve them by transforming them to singular integral equations. To this end, we introduce the dislocation density functions of the $k$th crack

$$\varphi_k(\theta) = \frac{1}{r_0}\frac{\partial}{\partial\theta}(\Delta u_k); \quad \psi_k(\theta) = \frac{1}{r_0}\frac{\partial}{\partial\theta}(\Delta v_k), \quad k = 1\text{–}n. \tag{26}$$

Then following the analysis similar to Part I of this two-part paper, we can rewrite (3.2) as

$$\begin{cases} \Delta\bar{u}_0 = -\dfrac{r_0}{2\pi}\displaystyle\sum_{l=1}^{n}\int_{a_l}^{b_l}\left(\zeta-\frac{a_l+b_l}{2}\right)\varphi_l(\zeta)\,\mathrm{d}\zeta, \quad \Delta\bar{u}_m = \frac{\mathrm{i}}{2\pi}\frac{r_0}{m}\displaystyle\sum_{l=1}^{n}\int_{a_l}^{b_l}\varphi_l(\zeta)\,\mathrm{e}^{\mathrm{i}m\zeta}\,\mathrm{d}\zeta \\ \Delta\bar{v}_0 = -\dfrac{r_0}{2\pi}\displaystyle\sum_{l=1}^{n}\int_{a_l}^{b_l}\left(\zeta-\frac{a_l+b_l}{2}\right)\psi_l(\zeta)\,\mathrm{d}\zeta, \quad \Delta\bar{v}_m = \frac{\mathrm{i}}{2\pi}\frac{r_0}{m}\displaystyle\sum_{l=1}^{n}\int_{a_l}^{b_l}\psi_l(\zeta)\,\mathrm{e}^{\mathrm{i}m\zeta}\,\mathrm{d}\zeta \end{cases} \tag{27}$$

which when substituted into eqn (24) yields

$$\begin{cases} \dfrac{\mathrm{i}}{2\pi}\displaystyle\sum_{l=1}^{n}\left[\int_{a_l}^{b_l}\varphi_l(\zeta)\sum_{m=-\infty}^{\infty}M_m^{(11)}\,\mathrm{e}^{\mathrm{i}m(\zeta-\theta)}\,\mathrm{d}\zeta+\int_{a_l}^{b_l}\psi_l(\zeta)\sum_{m=-\infty}^{\infty}M_m^{(12)}\,\mathrm{e}^{\mathrm{i}m(\zeta-\theta)}\,\mathrm{d}\zeta\right] = -\sigma(\theta) \\ \dfrac{\mathrm{i}}{2\pi}\displaystyle\sum_{l=1}^{n}\left[\int_{a_l}^{b_l}\varphi_l(\zeta)\sum_{m=-\infty}^{\infty}M_m^{(21)}\,\mathrm{e}^{\mathrm{i}m(\zeta-\theta)}\,\mathrm{d}\zeta+\int_{a_l}^{b_l}\psi_l(\zeta)\sum_{m=-\infty}^{\infty}M_m^{(22)}\,\mathrm{e}^{\mathrm{i}m(\zeta-\theta)}\,\mathrm{d}\zeta\right] = -\tau(\theta) \end{cases} \quad \theta\in(a_k,b_k) \tag{28}$$

with

$$M_0^{(st)} = \mathrm{i}\mu_0 r_0 N_0^{(st)}\left(\zeta-\frac{a_l+b_l}{2}\right); \quad M_m^{(st)} = \mu_0\frac{r_0}{m}N_m^{(st)}, \quad m\neq 0, s, t = 1, 2. \tag{29}$$

Considering the properties of Hankel functions $H_m(z)$ as $m\to\infty$ [cf. Abramowitz and Stegun (1965)], we have

$$\begin{cases} M_m^{(11)}, M_m^{(22)} \sim \mathrm{sgn}(m)\beta-\dfrac{\alpha}{m}+O(m^{-2}) \\ M_m^{(12)}, -M_m^{(21)} \sim \mathrm{i}\left(\alpha-\dfrac{\beta}{|m|}\right)+O(m^{-2}) \end{cases} \quad m\to\pm\infty \tag{30}$$

with

$$\alpha = \mu_0(1-\kappa_0^{-1}), \quad \beta = -\mu_0(1+\kappa_0^{-1}), \tag{31}$$

where $\kappa_0 = 1+2\mu_0(\lambda_0+\mu_0)^{-1} = 3-4\nu_0$ and $\nu_0$ represents the Poisson ratio of the matrix.

Introducing the auxiliary functions

$$\begin{cases} \bar{M}_m^{(st)} = M_m^{(st)}-\beta\,\mathrm{sgn}(m)+\dfrac{\alpha}{m} & s = t, m\neq 0 \\ \bar{M}_m^{(st)} = M_m^{(st)}+(-1)^s\mathrm{i}\left(\alpha-\dfrac{\beta}{|m|}\right) & s\neq t, m\neq 0 \end{cases} \tag{32}$$

assuming

$$P_{st}(\zeta,\theta)=\begin{cases}\dfrac{\mathrm{i}}{2\pi}\left\{\left[M_0^{(st)}+2\mathrm{i}\sum\limits_{m=1}^{\infty}\bar{M}_m^{(st)}\sin m(\zeta-\theta)\right]-\mathrm{i}\alpha[\pi\,\mathrm{sgn}(\zeta-\theta)-(\zeta-\theta)]\right\} & s=t\\ (-1)^s\dfrac{\mathrm{i}}{2\pi}\left\{\left[-\mathrm{i}\alpha+2\sum\limits_{m=1}^{\infty}\bar{M}_m^{(st)}\cos m(\zeta-\theta)\right]+2\mathrm{i}\beta\ln\left|2\sin\left(\dfrac{\zeta-\theta}{2}\right)\right|\right\} & s\neq t\end{cases}\tag{33}$$

and applying the relations

$$\begin{cases}\displaystyle\sum_{|m|=1}^{\infty}\mathrm{sgn}(m)\,\mathrm{e}^{\mathrm{i}m(\zeta-\theta)}=\mathrm{i}\cot\left(\frac{\zeta-\theta}{2}\right)\\ \displaystyle\sum_{|m|=1}^{\infty}\frac{1}{m}\mathrm{e}^{\mathrm{i}m(\zeta-\theta)}=\mathrm{i}\pi\,\mathrm{sgn}(\zeta-\theta)-\mathrm{i}(\zeta-\theta)\\ \displaystyle\sum_{|m|=1}^{\infty}\frac{1}{|m|}\mathrm{e}^{\mathrm{i}m(\zeta-\theta)}=-2\ln\left|2\sin\left(\frac{\zeta-\theta}{2}\right)\right|\\ \displaystyle\sum_{m=-\infty}^{\infty}\mathrm{e}^{\mathrm{i}m(\zeta-\theta)}=2\pi\sum_{m=\infty}^{\infty}\delta(\zeta-\theta-2\pi m)\end{cases}\tag{34}$$

we can transform eqn (28) into a set of singular integral equations of the second type with Hilbert kernels

$$\begin{cases}-\alpha\displaystyle\sum_{l=1}^{n}\psi_l(\theta)-\frac{\beta}{2\pi}\sum_{l=1}^{n}\int_{a_l}^{b_l}\varphi_l(\zeta)\cot\left(\frac{\zeta-\theta}{2}\right)\mathrm{d}\zeta+\sum_{l=1}^{n}\int_{a_l}^{b_l}[\varphi_l(\zeta)P_{11}+\psi_l(\zeta)P_{12}]\,\mathrm{d}\zeta=-\sigma(\theta)\\ \alpha\displaystyle\sum_{l=1}^{n}\varphi_l(\theta)-\frac{\beta}{2\pi}\sum_{l=1}^{n}\int_{a_l}^{b_l}\psi_l(\zeta)\cot\left(\frac{\zeta-\theta}{2}\right)\mathrm{d}\zeta+\sum_{l=1}^{n}\int_{a_l}^{b_l}[\varphi_l(\zeta)P_{21}+\psi_l(\zeta)P_{22}]\,\mathrm{d}\zeta=-\tau(\theta)\end{cases}\qquad\theta\in(a_k,b_k)\tag{35}$$

where $\varphi_k(\zeta)$ and $\psi_k(\zeta)$ should also satisfy the additional single-valued conditions

$$\int_{a_k}^{b_k}\varphi_k(\zeta)\,\mathrm{d}\zeta=0,\quad\int_{a_k}^{b_k}\psi_k(\zeta)\,\mathrm{d}\zeta=0.\tag{36}$$

Equations (35) and (36) can be solved by using the method presented by Erdogan and Gupta (1971) with a slight modification. In next section, we will solve them numerically for the case of $n=1$, i.e. for the case of an inclusion with a single debond.

## 4. SOLUTION OF THE SINGULAR INTEGRAL EQUATIONS

When $n=1$, by using the following substitutions

$$\begin{cases}\theta=c\xi+d,\zeta=c\eta+d\\ \Phi(\eta)=\varphi_1(c\eta+d),\Psi(\eta)=\psi_1(c\eta+d)\\ \bar{P}_{st}(\eta,\xi)=-\dfrac{1}{\mathrm{i}\beta}P_{st}(c\eta+d,c\xi+d)\end{cases}\tag{37}$$

with $c=(b_1-a_1)/2$ and $d=(b_1+a_1)/2$, eqns (34) and (35) become

$$\begin{bmatrix} 0 & -i\gamma \\ i\gamma & 0 \end{bmatrix}\begin{Bmatrix}\Phi(\xi)\\ \Psi(\xi)\end{Bmatrix}+\frac{c}{2\pi i}\int_{-1}^{1}\begin{bmatrix}1 & 0\\ 0 & 1\end{bmatrix}\begin{Bmatrix}\Phi(\eta)\\ \Psi(\eta)\end{Bmatrix}\cot\frac{c(\eta-\xi)}{2}d\eta$$

$$+c\int_{-1}^{1}\begin{bmatrix}\bar{P}_{11} & \bar{P}_{12}\\ \bar{P}_{21} & \bar{P}_{22}\end{bmatrix}\begin{Bmatrix}\Phi(\eta)\\ \Psi(\eta)\end{Bmatrix}d\eta=\frac{1}{i\beta}\begin{Bmatrix}\sigma(c\xi+d)\\ \tau(c\xi+d)\end{Bmatrix},\quad |\xi|<1 \tag{38}$$

and

$$\int_{-1}^{1}\begin{Bmatrix}\Phi(\eta)\\ \Psi(\eta)\end{Bmatrix}d\eta=0, \tag{39}$$

where $\gamma=\alpha/\beta$ is Dundurs parameter or oscillation parameter (Dundurs, 1969) which defines the oscillatory square-root singularity. When $v_0=1/2$, which means the elastic matrix is incompressible (i.e. P wave propagates at infinitely great speed), the Dundurs parameter vanishes and thus the oscillatory form of the stress singularity should also vanish. In this case, eqn (38) becomes a set of singular integral equations of the first kind.

To solve eqn (38), we must first uncouple its dominant parts. To this end, we introduce two new functions $f(\eta)$ and $g(\eta)$ which are related to $\Phi(\eta)$ and $\Psi(\eta)$ by

$$\begin{Bmatrix}\Phi(\eta)\\ \Psi(\eta)\end{Bmatrix}=[R]\begin{Bmatrix}f(\eta)\\ g(\eta)\end{Bmatrix} \tag{40}$$

with

$$[R]=\begin{bmatrix}i & -i\\ 1 & 1\end{bmatrix}. \tag{41}$$

Substitute eqn (40) into eqn (38) and then premultiply eqn (38) by $[R]^{-1}$. The dominant parts of eqn (38) will be uncoupled. Forthermore, if we consider that a Hilbert kernel and a Cauchy kernel have the same singularity, a set of standard Cauchy singular integral equations with uncoupled dominant parts is obtained

$$\begin{bmatrix}-\gamma & 0\\ 0 & \gamma\end{bmatrix}\begin{Bmatrix}f(\xi)\\ g(\xi)\end{Bmatrix}+\frac{1}{\pi i}\int_{-1}^{1}\begin{bmatrix}1 & 0\\ 0 & 1\end{bmatrix}\begin{Bmatrix}f(\eta)\\ g(\eta)\end{Bmatrix}\frac{d\eta}{\eta-\xi}+c\int_{-1}^{1}\begin{bmatrix}Q_{11} & Q_{12}\\ Q_{21} & Q_{22}\end{bmatrix}\begin{Bmatrix}f(\eta)\\ g(\eta)\end{Bmatrix}d\eta=\begin{Bmatrix}\bar{\sigma}(\xi)\\ \bar{\tau}(\xi)\end{Bmatrix},$$

$$|\xi|<1 \tag{42}$$

in which

$$\begin{bmatrix}Q_{11} & Q_{12}\\ Q_{21} & Q_{22}\end{bmatrix}=[R]^{-1}\begin{bmatrix}\bar{P}_{11} & \bar{P}_{12}\\ \bar{P}_{21} & \bar{P}_{22}\end{bmatrix}[R]+\frac{1}{2\pi i}\left[\cot\frac{c(\eta-\xi)}{2}-\frac{2}{c(\eta-\xi)}\right][I] \tag{43}$$

$$\begin{Bmatrix}\bar{\sigma}(\xi)\\ \bar{\tau}(\xi)\end{Bmatrix}=\frac{1}{i\beta}[R]^{-1}\begin{Bmatrix}\sigma(c\xi+d)\\ \tau(c\xi+d)\end{Bmatrix}, \tag{44}$$

with $[I]$ denoting the unit matrix. $f(\eta)$ and $g(\eta)$ should also satisfy

$$\int_{-1}^{1}\begin{Bmatrix}f(\eta)\\ g(\eta)\end{Bmatrix}d\eta=0. \tag{45}$$

According to the general theory of singular integral equations (Muskhelishvili, 1953), we know that the fundamental solution of eqn (42) is

$$\begin{Bmatrix} W_f(\xi) \\ W_g(\xi) \end{Bmatrix} = \begin{Bmatrix} (1-\xi)^{\alpha_1}(1+\xi)^{\beta_1} \\ (1-\xi)^{\beta_1}(1+\xi)^{\alpha_1} \end{Bmatrix} \tag{46}$$

with

$$\alpha_1 = -\tfrac{1}{2}-i\lambda, \quad \beta_1 = -\tfrac{1}{2}+i\lambda, \quad \lambda = \frac{1}{2\pi}\ln\left(\frac{1+\gamma}{1-\gamma}\right). \tag{47}$$

Hence, the approximate solution of eqn (42) may now be expressed as

$$\begin{Bmatrix} f(\xi) \\ g(\xi) \end{Bmatrix} = \sum_{j=0}^{\infty} \begin{bmatrix} W_f(\xi) & 0 \\ 0 & W_g(\xi) \end{bmatrix} \begin{Bmatrix} \bar{A}_j P_j^{(\alpha_1\beta_1)}(\xi) \\ \bar{B}_j P_j^{(\beta_1\alpha_1)}(\xi) \end{Bmatrix} \tag{48}$$

where $P_j^{(\alpha_1\beta_1)}(\xi)$ and $P_j^{(\beta_1\alpha_1)}(\xi)$ are Jacobi polynomials, $\bar{A}_j$ and $\bar{B}_j$ are to be determined.

Substituting eqn (48) into eqn (43) and using orthogonality relation of Jacobi polynomials (Erdogan and Gupta, 1971)

$$\int_{-1}^{1} W(\eta)P_i^{(ab)}(\eta)P_j^{(ab)}(\eta)\,d\eta = \begin{cases} 0, & i \neq j \\ \theta_j^{(ab)} = \dfrac{2^{a+b+1}\Gamma(j+a+1)\Gamma(j+b+1)}{j!(2j+a+b+1)\Gamma(j+a+b+1)}, & i = j \end{cases} \tag{49}$$

with $\Gamma(\ )$ representing Gamma function, we obtain

$$\bar{A}_0 = \bar{B}_0 = 0. \tag{50}$$

Subsequently, substituting eqn (48) into eqn (42), multiplying the first equation of eqn (42) by $W_f^{-1}(\xi)P_k^{(-\alpha_1-\beta_1)}(\xi)$, the second equation by $W_g^{-1}(\xi)P_k^{(-\beta_1-\alpha_1)}(\xi)$, and then integrating both equations over $\xi$ from $-1$ to 1, we have an infinite system of linear algebraic equations

$$\begin{cases} \dfrac{\sqrt{1-\gamma^2}}{2i}\theta_k^{(-\alpha_1-\beta_1)}\bar{A}_{k+1} + \displaystyle\sum_{j=1}^{\infty}[C_{kj}^{(11)}\bar{A}_j + C_{kj}^{(12)}\bar{B}_j] = F_k \\ \dfrac{\sqrt{1-\gamma^2}}{2i}\theta_k^{(-\beta_1-\alpha_1)}\bar{B}_{k+1} + \displaystyle\sum_{j=1}^{\infty}[C_{kj}^{(21)}\bar{A}_j + C_{kj}^{(22)}\bar{B}_j] = G_k \end{cases} \qquad k = 0, 1, 2 \ldots \tag{51}$$

where we have used eqns (49), (40), the following relation

$$-\gamma W_f(\xi)P_j^{(\alpha_1\beta_1)}(\xi) + \frac{1}{\pi i}\int_{-1}^{1} W_f(\eta)P_j^{(\alpha_1\beta_1)}(\eta)\frac{d\eta}{\eta-\xi} = \frac{\sqrt{1-\gamma^2}}{2i}P_{j-1}^{(-\alpha_1-\beta_1)}(\xi), \quad |\xi| < 1 \tag{52}$$

and the similar relation for $P_j^{(\beta_1\alpha_1)}(\xi)$.

The unknown coefficients $\bar{A}_j$ and $\bar{B}_j$ can be obtained by solving truncated version of eqn (51) in which $C_{kj}^{(st)}(s, t = 1, 2)$, $F_k$ and $G_k$ are given in the Appendix.

## 5. DYNAMIC STRESS INTENSITY FACTORS AND RIGID BODY MOTION OF THE INCLUSION

We define the dynamic stress intensity factors (DSIFs) $K_{\mathrm{I}}$ and $K_{\mathrm{II}}$ by analogy with the definition of the static stress intensity factors (SSIFs) given by Erdogan and Gupta (1971). However, one may note that the DSIFs are complex and thus they can not be calculated by the method of Erdogan and Gupta (1971). Here we present another method to compute the DSIFs.

Denote $\sigma_r(r_0,\theta)$ and $\tau_{r\theta}(r_0,\theta)$ as the stresses on the bonded region and define the equivalent stress components $\sigma_r^{(e)}(r_0,\xi)$ and $\tau_{r\theta}^{(e)}(r_0,\xi)$ as

$$\begin{Bmatrix}\sigma_r^{(e)}(r_0,\xi)\\ \tau_{r\theta}^{(e)}(r_0,\xi)\end{Bmatrix}=\frac{1}{i\beta}[R]^{-1}\begin{Bmatrix}\sigma_r(r_0,\theta)\\ \tau_{r\theta}(r_0,\theta)\end{Bmatrix}. \tag{53}$$

The dominant parts of the equivalent stresses may be written as

$$\begin{Bmatrix}\sigma_r^{(e)}(r_0,\xi)\\ \tau_{r\theta}^{(e)}(r_0,\xi)\end{Bmatrix}\sim\frac{1}{\pi i}\int_{-1}^{1}\begin{Bmatrix}f(\eta)\\ g(\eta)\end{Bmatrix}\frac{d\eta}{\eta-\xi},\quad |\xi|>1. \tag{54}$$

It can be shown that the equivalent stresses have the following behavior at the crack tips

$$\begin{Bmatrix}\sigma_r^{(e)}(r_0,\xi)\\ \tau_{r\theta}^{(e)}(r_0,\xi)\end{Bmatrix}\approx\begin{Bmatrix}K_{Ib_1}^{(e)}(r_0c)^{-1/2}(\xi-1)^{\alpha_1}(\xi+1)^{\beta_1}\\ K_{IIb_1}^{(e)}(r_0c)^{-1/2}(\xi-1)^{\beta_1}(\xi+1)^{\alpha_1}\end{Bmatrix}\quad \xi\to 1^+ \tag{55}$$

$$\begin{Bmatrix}\sigma_r^{(e)}(r_0,\xi)\\ \tau_{r\theta}^{(e)}(r_0,\xi)\end{Bmatrix}\approx\begin{Bmatrix}K_{Ia_1}^{(e)}(r_0c)^{-1/2}(1-\xi)^{\alpha_1}(-\xi-1)^{\beta_1}\\ K_{IIa_1}^{(e)}(r_0c)^{-1/2}(1-\xi)^{\beta_1}(-\xi-1)^{\alpha_1}\end{Bmatrix}\quad \xi\to -1^- \tag{56}$$

where $K_{Ib_1}^{(e)}, K_{Ia_1}^{(e)}, K_{IIb_1}^{(e)}$ and $K_{IIa_1}^{(e)}$ denote the equivalent DSIFs.

Substituting eqn (48) into eqn (54), we can derive

$$\begin{Bmatrix}K_{Ib_1}^{(e)}\\ K_{IIb_1}^{(e)}\end{Bmatrix}=i\sqrt{(1-\gamma^2)r_0c}\sum_{j=1}^{\infty}\begin{Bmatrix}\bar{A}_jP_j^{(\alpha_1\beta_1)}(1)\\ \bar{B}_jP_j^{(\beta_1\alpha_1)}(1)\end{Bmatrix} \tag{57}$$

$$\begin{Bmatrix}K_{Ia_1}^{(e)}\\ K_{IIa_1}^{(e)}\end{Bmatrix}=i\sqrt{(1-\gamma^2)r_0c}\sum_{j=1}^{\infty}\begin{Bmatrix}\bar{A}_jP_j^{(\alpha_1\beta_1)}(-1)\\ \bar{B}_jP_j^{(\beta_1\alpha_1)}(-1)\end{Bmatrix} \tag{58}$$

where we have used the relations

$$\begin{cases}\dfrac{1}{\pi i}\displaystyle\int_{-1}^{1}W_f(\eta)P_j^{(\alpha_1\beta_1)}(\eta)\frac{d\eta}{\eta-\xi}=-(1+\gamma)[-\bar{W}_fP_j^{(\alpha_1\beta_1)}(\xi)+G_{fj}^{\infty}(\xi)]\\ \dfrac{1}{\pi i}\displaystyle\int_{-1}^{1}W_g(\eta)P_j^{(\beta_1\alpha_1)}(\eta)\frac{d\eta}{\eta-\xi}=-(1-\gamma)[-\bar{W}_gP_j^{(\beta_1\alpha_1)}(\xi)+G_{gj}^{\infty}(\xi)]\end{cases}\quad |\xi|>1 \tag{59}$$

with

$$\bar{W}_f(\xi)=i\sqrt{\frac{1-\gamma}{1+\gamma}}|\xi-1|^{\alpha_1}|\xi+1|^{\beta_1},\quad \bar{W}_g(\xi)=i\sqrt{\frac{1-\gamma}{1+\gamma}}|\xi-1|^{\beta_1}|\xi+1|^{\alpha_1} \tag{60}$$

and $G_{fj}^{\infty}(\xi)$ and $G_{gj}^{\infty}(\xi)$ being the dominant parts of $W_f(\xi)P_j^{(\alpha_1\beta_1)}(\xi)$ and $W_g(\xi)P_j^{(\beta_1\alpha_1)}(\xi)$ as $\xi\to\infty$.

The real DSIFs can be calculated by

$$\begin{Bmatrix}K_{Ix}\\ K_{IIx}\end{Bmatrix}=i\beta[R]\begin{Bmatrix}K_{Ix}^{(e)}\\ K_{IIx}^{(e)}\end{Bmatrix}, \tag{61}$$

where $x=a_1$ or $b_1$.

The amplitudes of the rigid body translations (RBTs) of the inclusion in $x$- and $y$-direction denoted by $U$ and $V$ and the amplitude of the rigid body rotation (RBR) denoted by $\Theta$ may be obtained from eqn (11) where $U^{(0)}$, $V^{(0)}$, and $\Theta^{(0)}$ may be found in Pao and Mow (1973) and $U^{(1)}$, $V^{(1)}$ and $\Theta^{(1)}$ can be calculated from eqns (13), (22), (27), (27), (37), (40) and (38). The detailed analysis will not be presented here.

## 6. SCATTERED FAR FIELD PATTERN AND SCATTERING CROSS-SECTION

By using the properties of Hankel functions in the far field (Abramowitz and Stegun, 1965), the scattered far field displacements can be expressed as the following asymptotic expressions

$$\begin{cases} u_0^{(0)}(r,\theta)+u_0^{(1)}(r,\theta) \approx \mathrm{i}K_{\mathrm{L}0}\sqrt{\dfrac{8\pi}{K_{\mathrm{L}0}r}}\,\mathrm{e}^{\mathrm{i}\left(K_{\mathrm{L}0}r-\frac{\pi}{4}\right)}F_r(\theta,\theta_0) \\ v_0^{(0)}(r,\theta)+v_0^{(1)}(r,\theta) \approx \mathrm{i}K_{\mathrm{T}0}\sqrt{\dfrac{8\pi}{K_{\mathrm{T}0}r}}\,\mathrm{e}^{\mathrm{i}\left(K_{\mathrm{T}0}r-\frac{\pi}{4}\right)}F_\theta(\theta,\theta_0) \end{cases}, \quad r\to+\infty \tag{62}$$

where $F_r(\theta,\theta_0)=F_r^{(0)}(\theta,\theta_0)+F_r^{(1)}(\theta,\theta_0)$ and $F_\theta(\theta,\theta_0)=F_\theta^{(0)}(\theta,\theta_0)+F_\theta^{(1)}(\theta,\theta_0)$. $F_r^{(0)}(\theta,\theta_0)$ and $F_\theta^{(0)}(\theta,\theta_0)$ are the scattered far field patterns for a perfectly bonded inclusion [cf. Pao and Mow (1973)]. $F_r^{(1)}(\theta,\theta_0)$ and $F_\theta^{(1)}(\theta,\theta_0)$ are those due to debonding which, by considering eqn (8), can be written as

$$\begin{cases} F_r^{(1)}(\theta,\theta_0)=\dfrac{1}{2\pi}\displaystyle\sum_{m=-\infty}^{\infty}(-\mathrm{i})^m A_m\,\mathrm{e}^{-\mathrm{i}m\theta} \\ F_\theta^{(1)}(\theta,\theta_0)=\dfrac{1}{2\pi}\displaystyle\sum_{m=-\infty}^{\infty}(-\mathrm{i})^m B_m\,\mathrm{e}^{-\mathrm{i}m\theta} \end{cases}. \tag{63}$$

$A_m$ and $B_m$ in eqn (63) can be computed from eqns (21), (22), (27), (37), (40) and (48). We will not give here the detailed analysis.

The total scattered energy flux is defined as (Pao and Mow, 1973):

$$\langle P^s\rangle=\frac{\omega}{2}\,\mathrm{Im}\int_S[(u_0^{(0)}+u_0^{(1)})^*\cdot(\sigma_{r0}^{(0)}+\sigma_{r0}^{(1)})+(v_0^{(0)}+v_0^{(1)})^*\cdot(\tau_{r\theta0}^{(0)}+\tau_{r\theta0}^{(1)})]\,\mathrm{d}s \tag{64}$$

with the asterisk representing conjugation. $S$ is chosen to be a unit-length cylindrical surface with radius of infinitely large. Considering the asymptotic expressions of the scattered far field displacements given by eqn (62), we have

$$\langle P^s\rangle=4\pi\omega\mu_0K_{T0}^2\int_{-\pi}^{\pi}[|F_r^{(0)}+F_r^{(1)}|^2+|F_\theta^{(0)}+F_\theta^{(1)}|^2]\,\mathrm{d}\theta. \tag{65}$$

The total scattering cross-section (SCS) is defined as (Pao and Mow, 1973):

$$\sigma(\omega)=\frac{\langle P^s\rangle}{\langle \dot{e}_0\rangle} \tag{66}$$

where $\langle \dot{e}_0\rangle$ is the time average of the incident flux which can be expressed as (Pao and Mow, 1973):

$$\langle \dot{e}_0 \rangle = \frac{\omega}{2} \mu_0 K_{L0} K_{T0}^2 |A|^2 \tag{67}$$

for the incident P wave, or:

$$\langle \dot{e}_0 \rangle = \frac{\omega}{2} \mu_0 K_{T0}^3 |A|^2 \tag{68}$$

for the incident SV wave.

The SCS can also be calculated by following the elasto-dynamic optical theorem [cf. Yang and Norris (1992)], which may be used as a check on the numerical computations.

## 7. THE LONG WAVELENGTH LIMIT

It has been demonstrated by Yang and Norris (1991, 1992) that the dynamic results reduce to the relevant quasistatic ones in this long wavelength limit. In Part I we have derived the explicit static solution from the singular integral equations for SH-wave incidence as the frequency reduces to zero. Here we will consider this limit for P- and SV-wave incidence. We assume $K_{T0} r_0 \ll 1$ and $K_{L0} r_0 = O(K_{T0} r_0)$. Then the kernel $P_{st}(\zeta, \theta)$ in eqn (36) may be written as

$$\begin{aligned} P_{22}(\zeta, \theta) &= P_{11}(\zeta, \theta) - \frac{\mu_0}{\pi} \left( \zeta - \frac{a_l + b_l}{2} \right) \\ &= \frac{\alpha}{2\pi} [\pi \operatorname{sgn}(\zeta - \theta) - (\zeta - \theta)] + \frac{2}{\pi} [2\mu_0 - (\alpha - \beta)] \sin(\zeta - \theta) + o(1) \\ P_{12}(\zeta, \theta) &= -P_{21}(\zeta, \theta) \\ &= \frac{\alpha}{2\pi} - \frac{\beta}{\pi} \ln \left| 2 \sin \left( \frac{\zeta - \theta}{2} \right) \right| - \frac{2}{\pi} [2\mu_0 - (\alpha - \beta)] \cos(\zeta - \theta) + o(1). \end{aligned} \tag{69}$$

Similarly, $\sigma(\theta)$ and $\tau(\theta)$ become

$$\begin{cases} \sigma(\theta) = \tau_0 \{1 + (1 - \kappa_0^{-1}) \cos 2(\theta - \theta_0)] + o(1)\} \\ \tau(\theta) = \tau_0 \{(1 - \kappa_0^{-1}) \sin 2(\theta - \theta_0) + o(1)\} \end{cases} \tag{70}$$

where $\tau_0 = -\mu_0 K_{T0}^2 A$.

If we consider the case of $n = 1$ (i.e. the case of an inclusion with one debond), and assume $b_1 = -a_1 = c$, we can precisely follow the analysis of Section 4 by replacing $P_{st}(\zeta, \theta)$, $\sigma(\theta)$ and $\tau(\theta)$ with eqns (69) and (70). Note please, that $\varphi_1(\zeta)$ and $\psi_1(\zeta)$ or $\Phi(\eta)$ and $\Psi(\eta)$ are all real. Therefore eqn (40) may be rewritten as

$$f(\eta) = \tfrac{1}{2}[\Psi(\eta) - \mathrm{i}\Phi(\eta)] = g^*(\eta) \tag{71}$$

where asterisk represents the complex conjugation. Since $P_{st}(\zeta, \theta)$ given by eqn (69) and $\sigma(\theta)$ and $\tau(\theta)$ by eqn (70) are all real, we have

$$Q_{12} = -Q_{12}^*, \quad Q_{11} = -Q_{22}^*, \quad \bar{\sigma} = -\bar{\tau}^*. \tag{72}$$

Then the singular integral equation group given by eqn (42) may be replaced by a single equation as follows

$$-\gamma f(\xi)+\frac{1}{\pi i}\int_{-1}^{1}\frac{f(\eta)}{\eta-\xi}d\eta+c\int_{-1}^{1}[f(\eta)Q_{11}+f^{*}(\eta)Q_{12}]\,d\eta=\bar{\sigma}(\xi). \tag{73}$$

It is quite difficult to obtain the analytical solution of eqn (73) just like we did in Part I for SH case. Here we will solve it numerically by the method of Erdogan and Gupta (1971).

The definition of stress intensity factors described in Section 4 may also be expressed, for crack tip $\theta=+c$, as

$$K_{I}^{+}+iK_{II}^{+}=\lim_{\theta\to+c^{+}}\sqrt{r_0 c}(\theta/c-1)^{-\alpha_1}(1+\theta/c)^{-\beta_1}(\sigma_r+i\tau_{r\theta}). \tag{74}$$

Following the analysis of Erdogan and Gupta (1971), we have

$$K_{I}^{+}+iK_{II}^{+}=-2i\beta\sqrt{(1-\gamma)^2 r_0 c}\lim_{\xi\to1^{+}}[W_f^{-1}(\xi)f(\xi)]. \tag{75}$$

If we consider the physical meaning of the incident fields as $K_{T0}r_0\to0$, that is, the incident stresses give precisely the biaxial loadings at infinity: $\tau_0$ in $\theta_0$-direction and $\tau_0\nu_0/(1-\nu_0)$ perpendicular to $\theta_0$-direction, we may say that the above $K_{I}^{+}$ and $K_{II}^{+}$ coincide exactly with the SSIFs presented by Toya (1974) for an arc-shaped interface crack subjected to above biaxial loadings. For a rigid inclusion, the results of Toya (1974) state

$$\sigma_r+i\tau_{r\theta}=-\tfrac{1}{2}(1+\kappa_0)P(\theta)\chi^{+}(\theta) \tag{76}$$

where

$$\chi^{+}(\theta)=(e^{i\theta}-e^{ic})^{-1/2-i\lambda}(e^{i\theta}-e^{-ic})^{-1/2+i\lambda} \tag{77}$$

with $\lambda$ given by eqn (47) which differs from $\lambda$ in Toya (1974) by a negative sign. $P(\theta)$ is

$$\begin{aligned}P(\theta)=&[iH-\tfrac{1}{2}(N_\infty+T_\infty)][\exp(i\theta)-(\cos\alpha-2\lambda\sin\alpha)]\\&+(N_\infty-T_\infty)[(\cos\alpha+2\lambda\sin\alpha)\exp(-i\theta)-\exp(-2i\theta)]\exp[2i\theta_0-2\lambda(\alpha-\pi)]\end{aligned} \tag{78}$$

where

$$H=\frac{(1+4\lambda^2)(N_\infty-T_\infty)\sin^2\alpha\cos2\theta_0}{2\{1+(\cos\alpha-2\lambda\sin\alpha)\exp[-2\lambda(\pi-\alpha)]\}} \tag{79}$$

and $T_\infty=\tau_0$, $N_\infty=T_\infty\nu_0/(1-\nu_0)$. The SSIFs at crack tip $\theta=+c$ are

$$K_{I}^{+}+iK_{II}^{+}=-\tfrac{1}{2}(1+\kappa_0)P(c)(e^{ic})^{1/2+i\lambda}(c^{-1}\sin c)^{1/2-i\lambda}\sqrt{r_0/c}. \tag{80}$$

The comparison between the numerical results of eqn (75) and the analytical results of eqn (80) will be displayed in Section 9 and good agreement may be found.

In above analysis we assume that the incident wave is P wave. For an incident SV wave, $\sigma(\theta)$ and $\tau(\theta)$ may be expressed, in long wavelength limit, as

$$\begin{cases}\sigma(\theta)=\tau_0(1+\kappa_0^{-1})\sin2(\theta-\theta_0)+o(1)\\ \tau(\theta)=\tau_0(1+\kappa_0^{-1})\cos2(\theta-\theta_0)+o(1)\end{cases} \tag{81}$$

with $\tau_0=-\mu_0 K_{T0}^2 A$. The DSIFs as $K_{T0}r_0\to0$ can also be obtained numerically from eqn (75). In this limiting situation, the incident SV wave yields in-plane shear stress $-\tau_0$ at infinity, which is inclined at the angle $\theta_0$, and also results in the rotation $\Theta_\infty=-K_{T0}^2 A/2$

at infinity. Therefore the relevant SSIFs may be obtained from eqn (80) by setting $\theta_0 = \theta_0 + 45^\circ$ and $N_\infty = -T_\infty = \tau_0$.

It is seen clearly from eqn (73) that as $K_{T0}r_0 \to 0$, $r_0^2\varphi_1(\zeta)$ and $r_0^2\psi_1(\zeta)$ are of order $A(K_{T0}r_0)^2$. Therefore

$$F_\theta^{(1)}/A, \quad F_r^{(1)}/A \approx O((K_{T0}r_0)^2) \tag{82}$$

and

$$\frac{U^{(1)}}{iK_{L0}A}, \quad \frac{V^{(1)}}{iK_{L0}A} \approx O(K_{T0}r_0) \tag{83}$$

which mean that for very low frequency, the presence of the debond only produces a change of order $(K_{T0}r_0)^2$ in the far field displacements and a change of order $(K_{T0}r_0)^1$ in the RBT, while the rotation of the inclusion in this limit case behaves like

$$\frac{\Theta^{(0)} + \Theta^{(1)}}{-K_{T0}^2 A/2} = 1 + \frac{1}{2\pi}\int_{-c}^{c} \zeta\psi(\zeta)\,d\zeta + o(1) \tag{84}$$

which should be the same as the static rotation presented by Toya (1974) as

$$\Theta = \frac{(1+\kappa_0)H}{4\mu_0} + \Theta_\infty \tag{85}$$

with $H$ given by eqn (79).

## 8. THE SMALL DEBOND LIMIT

Yang and Norris (1991) have obtained the explicit solution in this limit for SH-wave incidence when $K_{T0}r_0 = O(1)$. In Part I we have discussed this limit by allowing for arbitrary frequencies, and the results of Yang and Norris (1991) have been obtained as a special case. For P- and SV-wave incidence, the analysis will be much more difficult and we will focus our attention on the case of $K_{T0}r_0 = O(1)$ for simplicity. It is also assumed $K_{L0}r_0 = O(K_{T0}r_0)$ and only the case of one debond is considered. Set $b_1 = -a_1 = c$. Then under the substitutions $\zeta = c\eta$, $\theta = c\xi$, $\Phi(\eta) = \varphi_1(c\eta)$ and $\Psi(\eta) = \psi_1(c\eta)$, eqn (28) becomes

$$\begin{cases} \dfrac{ic}{2\pi}\left[\displaystyle\int_{-1}^{1} \Phi(\eta) \sum_{m=-\infty}^{\infty} \bar{M}_m^{(11)} e^{imc(\eta-\xi)}\,d\eta + \int_{-1}^{1} \Psi(\eta) \sum_{m=-\infty}^{\infty} \bar{M}_m^{(12)} e^{imc(\eta-\xi)}\,d\eta\right] = -\sigma(c\xi) \\ \dfrac{ic}{2\pi}\left[\displaystyle\int_{-1}^{1} \Phi(\eta) \sum_{m=-\infty}^{\infty} \bar{M}_m^{(21)} e^{imc(\eta-\xi)}\,d\eta + \int_{-1}^{1} \Psi(\eta) \sum_{m=-\infty}^{\infty} \bar{M}_m^{(22)} e^{imc(\eta-\xi)}\,d\eta\right] = -\tau(c\xi) \end{cases} \quad |\xi| < 1 \tag{86}$$

where $\bar{M}_0^{(st)} = ic\mu_0 r_0 N_0^{(st)}\eta$ and $\bar{M}_m^{(st)} = \mu_0 r_0 m^{-1} N_m^{(st)}$ with $N_m^{(st)}$ given in the Appendix. Set $p = mc$. We have for $c \ll 1$

$$\sum_{m=-\infty}^{\infty} \bar{M}_m^{(st)} e^{imc(\eta-\xi)} = \int_{-\infty}^{\infty} c^{-1} \bar{M}_{p/c}^{(st)} e^{ip(\eta-\xi)}\,dp \equiv I_{st}. \tag{87}$$

Considering the properties of Hankel functions for large order (Abramowitz and Stegun, 1965), we have

$$\bar{M}^{(st)}_{p/c} = \operatorname{sgn}(p)\beta + o(1), \quad s = t \tag{88}$$
$$= (-1)^t \mathrm{i}\alpha + o(1), \quad s \neq t$$

with $\alpha$ and $\beta$ given by eqn (31). Substitution of eqn (85) into eqn (87) yields

$$I_{11} = I_{22} = c^{-1}\beta \int_{-1}^{1} \operatorname{sgn}(p)\, \mathrm{e}^{\mathrm{i}p(\eta-\xi)}\, \mathrm{d}p = \frac{2\mathrm{i}\beta c^{-1}}{\eta-\xi}, \tag{89a}$$

$$I_{12} = -I_{21} = \mathrm{i}c^{-1}\alpha \int_{-1}^{1} \mathrm{e}^{\mathrm{i}p(\eta-\xi)}\, \mathrm{d}p = 2\mathrm{i}c^{-1}\alpha\pi\delta(\eta-\xi). \tag{89b}$$

For very small $c$, $\sigma(c\xi)$ and $\tau(c\xi)$ behave like $\sigma(0)+o(1)$ and $\tau(0)+o(1)$. Therefore eqn (86) becomes

$$\begin{cases} -\alpha\Psi(\xi) - \dfrac{\beta}{\pi}\displaystyle\int_{-1}^{1} \frac{\Phi(\eta)}{\eta-\xi}\mathrm{d}\eta = -\sigma(0) \\ \alpha\Phi(\xi) - \dfrac{\beta}{\pi}\displaystyle\int_{-1}^{1} \frac{\Psi(\eta)}{\eta-\xi}\mathrm{d}\eta = -\tau(0) \end{cases}, \quad |\xi| < 1 \tag{90}$$

which can be solved by following the method presented in Section 4. In fact it has an explicit solution which may be written as [cf. Erdogan and Gupta (1971)]

$$\begin{cases} \Phi(\xi) = \mathrm{i}f(\xi) - \mathrm{i}g(\xi) \\ \Psi(\xi) = f(\xi) + g(\xi) \end{cases} \tag{91}$$

where

$$\begin{cases} f(\xi) = \dfrac{2\mathrm{i}\bar{\sigma}(0)}{\sqrt{1-\gamma^2}} W_f(\xi) P_1^{(\alpha_1\beta_1)}(\xi) \\ g(\xi) = -\dfrac{2\mathrm{i}\bar{\tau}(0)}{\sqrt{1-\gamma^2}} W_g(\xi) P_1^{(\beta_1\alpha_1)}(\xi) \end{cases} \tag{92}$$

with

$$\begin{cases} \bar{\sigma}(0) = -\dfrac{1}{2\beta}[\sigma(0) + \mathrm{i}\tau(0)] \\ \bar{\tau}(0) = -\dfrac{1}{2\beta}[\sigma(0) - \mathrm{i}\tau(0)] \end{cases} \tag{93}$$

and $W_f(\xi)$ and $W_g(\xi)$ given by eqn (46).

The DSIFs defined in Section 5 are

$$K_{\mathrm{I}} = -[\sigma(0) + 2\lambda\tau(0)]\sqrt{b}; \quad K_{\mathrm{II}} = [2\lambda\sigma(0) - \tau(0)]\sqrt{b} \tag{94a,b}$$

at the crack tip $\theta = +c$ (i.e. tip $b_1$). In the above equation, $b = r_0 c$.

Comparing eqns (94a,b) with the results of Erdogan and Gupta (1971), one may find that eqns (94a,b) are actually the SSIFs of a flat interface crack between a rigid half-space and an elastic one subjected to tractive loading $\sigma(0)$ and in-plane shear loading $\tau(0)$ at infinity. This conclusion is similar to that for the SH case.

Following the analysis of Part I, we find that the presence of a small debond produces changes of order $c^2$ in the scattered far field displacements and motion of the inclusion.

## 9. NUMERICAL RESULTS AND DISCUSSION

The SCS, DSIF, RBT and RBR have been computed for rigid/epoxy combination of inclusion and matrix with one debond. The shear modulus, Poisson ratio and mass density of epoxy ($\mu_0$, $\nu_0$, $\rho_0$) are taken to be the same as those given by Yang and Norris (1992) and the mass density of the rigid inclusion is assumed to be the same as that of glass. We have demonstrated in Part I that this combination of inclusion and matrix may provide a good approximation for the glass/epoxy combination.

The DSIFs for P-wave incidence in 0°-direction and RBR for SV-wave incidence in the same direction have been computed in the long wavelength limit and compared with the static solutions of Toya (1974). They are displayed in Figs 2 and 3, respectively. The computations were performed by expanding $f(\eta)$ in eqn (73) as a series in approprate Jacobi polynomials [cf. Erdogan and Gupta (1971)]. For a smaller debond, 6 or 8 terms were included in the series and for a larger one, 8 or 10 terms were used. The comparison shows good agreement between the results of the present study and those of Toya (1974).

The normalized first and second DSIFs versus $K_{T0}r_0$ (which varies from 0 to 5) are shown in Fig. 4 for P-wave incidence with $\alpha = 150°$, $\theta° = 0°$ and 180°. As we expected, a resonance peak appears at a low frequency. Its mechanism is similar to that encounted in the SH case. The resonances at higher frequencies reported by Yang and Norris (1992) for the "glass"/epoxy (where "glass" has been adjusted so that the Dundur's parameter is zero) do not appear. This means that the effect of the surface waves is negligible in the rigid-inclusion case (at least when $K_{T0}r_0 < 5$). The results of the DSIFs for SV-wave incidence with the same geometric configuration are presented in Fig. 5. The resonance peaks are sharper and occur at lower frequency than those in Fig. 4. This characteristic of resonances

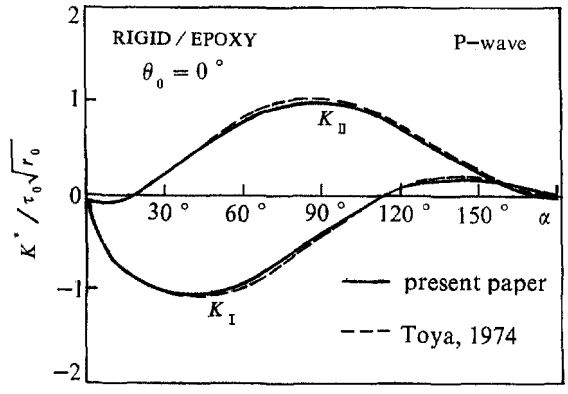


Fig. 2. Comparison of the DSIFs in the long wavelength limit with the SSIFs calculated from Toya (1974) for P-wave incidence in 0°-direction ($\theta_0 = 0°$).

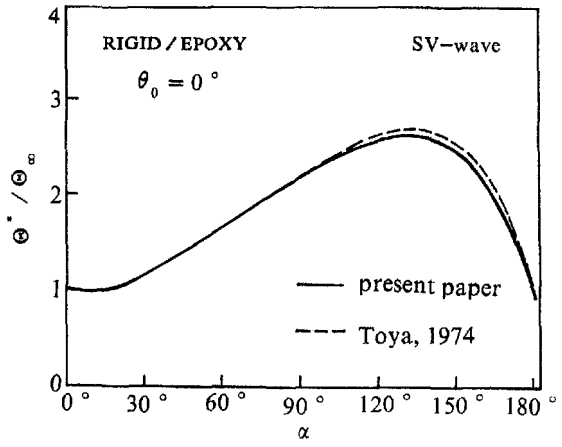


Fig. 3. Comparison of the RBR in the long wavelength limit with the static values from Toya (1974) for SV-wave incidence in 0°-direction ($\theta_0 = 0°$).

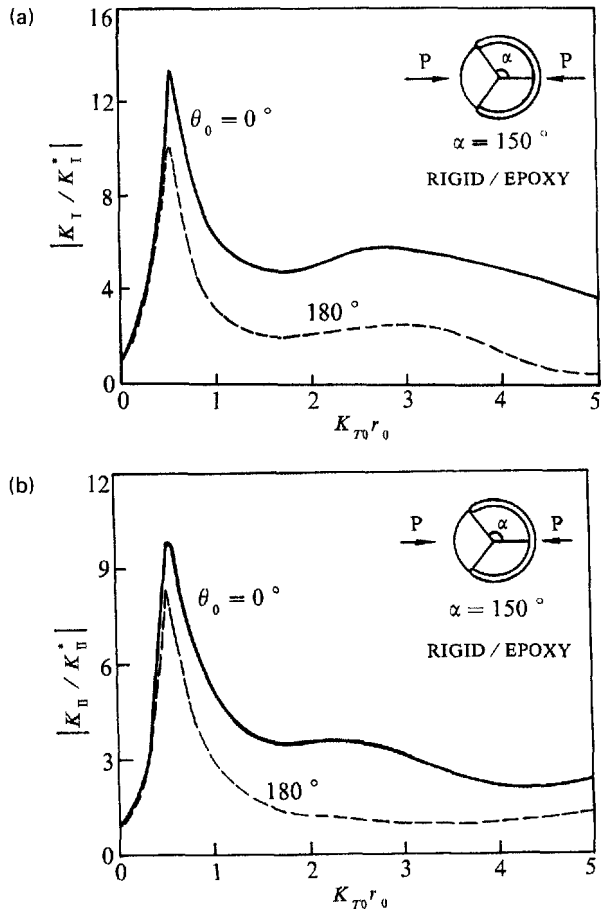


Fig. 4. The absolute-valued DSIFs normalized with the static value vs $K_{T0}r_0$ for the P-wave incidence in 0°- and 180°-direction with $\alpha = 150°$. (a) The first DSIF. (b) The second DSIF.

may be shown clearly by the motion of the inclusion and will be discussed later. In Figs 4–7, it is shown that the DSIFs for $\theta_0 = 0°$ are higher than those for $\theta_0 = 180°$. This has been explained in Part I.

The numerical results of the DSIFs for a small debond ($\alpha = 2°$) are plotted in Fig. 6 against $K_{T0}r_0$ for P-wave incidence. The approximate solution in the small debond limit given by (94a) for the first DSIF is shown by dotted curves for comparison. It is seen that eqn (94) may provide a good approximation when $K_{T0}r_0 < 5$.

The SCS versus $K_{T0}r_0$ for P-wave incidence is illustrated in Fig. 7 for $\theta_0 = 0°$ and in Fig. 8 for $\theta_0 = 90°$. The low-frequency resonance and its dependence upon the debond size are very similar to what we have shown in SH case. However, unlike in SH case, the incident angle $\theta_0$ has a significant effect on the resonant frequence of the SCS. For an inclusion with a debond symmetric about the $x$-axis, the incident P-wave in $y$-direction ($\theta_0 = 90°$) yields a stronger resonance at a lower frequency than that in $x$-direction ($\theta_0 = 0°$), especially when the debond is larger. Figure 9 illustrates the curves of the SCS versus $K_{T0}r_0$ for SV-wave incidence in $x$-direction ($\theta_0 = 0°$), which look very much like those in Fig. 8, except that the resonance peaks in Fig. 9 are sharper and higher. All these characteristics of the resonance are closely related to the motion of the inclusion which will be discussed next in detail.

The in-plane motion of the rigid inclusion may be described by the rigid body translations (RBTs) along $x$- and $y$-axis and rigid body rotation (RBR) around $z$-axis which are denoted by $U$, $V$, and $\Theta$, respectively. The RBTs ($U$, $V$) and RBR ($\Theta$) have been computed for three situations: (i) P-wave incidence in $x$-direction ($\theta_0 = 0°$); (ii) P-wave incidence in $y$-direction ($\theta_0 = 90°$); and (iii) SV-wave incidence in $x$-direction ($\theta_0 = 0°$). The debond is located symmetrically about $x$-axis. The normalized results are displayed in Figs 10–12 in

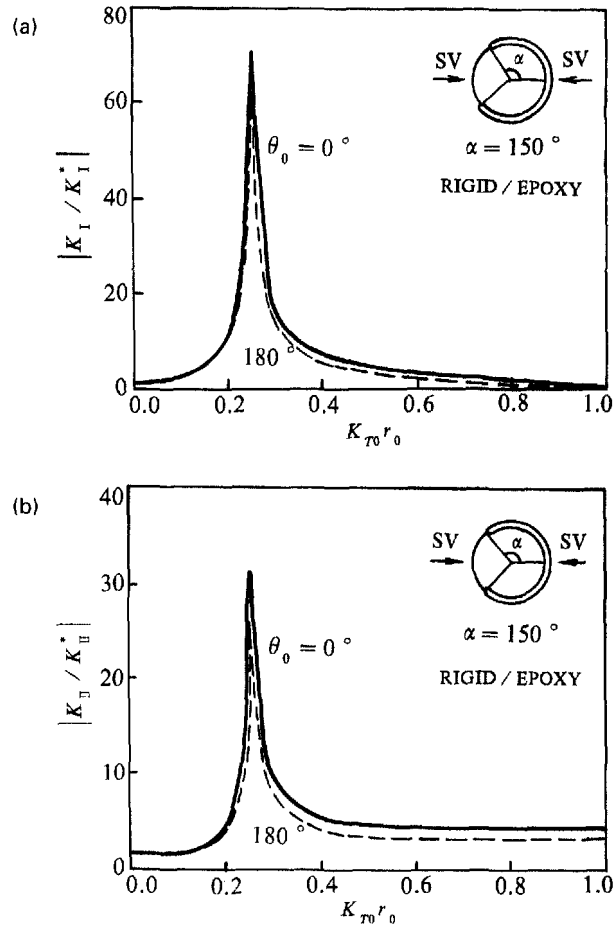


Fig. 5. The absolute-valued DSIFs normalized with the static value versus $K_{T0}r_0$ for the SV wave incidence in 0°- and 180°-direction with $\alpha = 150°$. (a) The first DSIF. (b) The second DSIF.

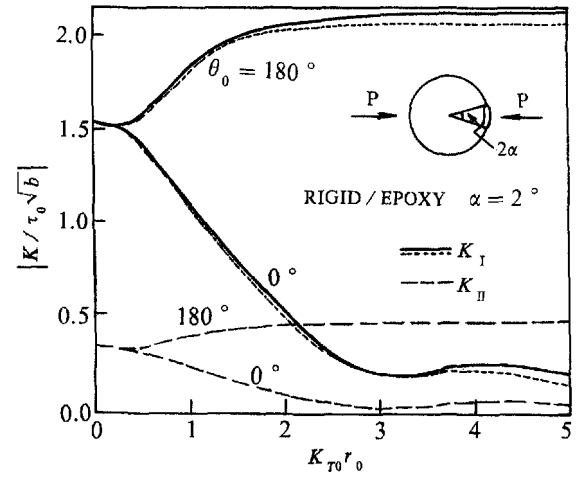


Fig. 6. The absolute-valued DSIFs normalized with $\tau_0\sqrt{b}$ for a small debond ($\alpha = 2°$) with $\theta_0 = 0°$ and 180°, P-wave incidence. The dotted curve is from the asymptotic approximation of eqn (94a) for small debond limit.

absolute values. In the first case, only the motion in $x$-direction exists because of the symmetry about $x$-axis, while in the last case, it vanishes because of the antisymmetry. In the second case, all three kinds of motion take place in a full dynamic state even though the motion in $x$-direction and rotation vanish in the quasi-static limit. The motion of the

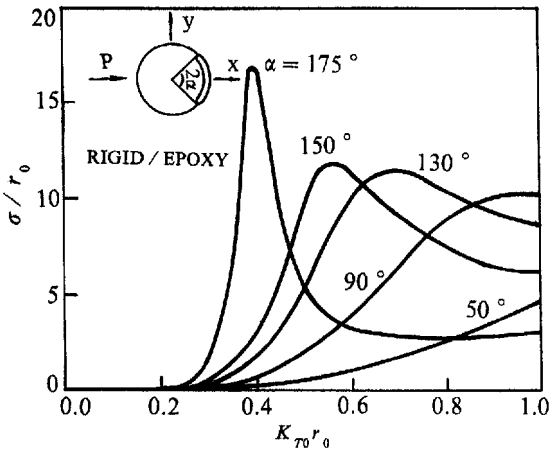


Fig. 7. The SCS vs $K_{T0}r_0$ for the $P$-wave incidence in $x$-direction ($\theta_0 = 0°$) with $\alpha = 170°$, 150°, 130°, 90°, and 50°.

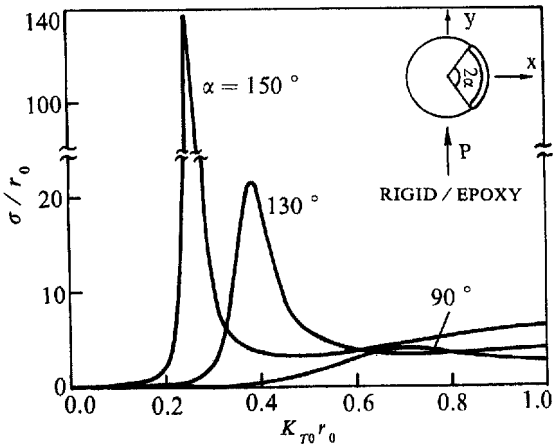


Fig. 8. The SCS vs $K_{T0}r_0$ for P-wave incidence in $y$-direction ($\theta_0 = 90°$) with $\alpha = 150°$, 130°, and 90°.

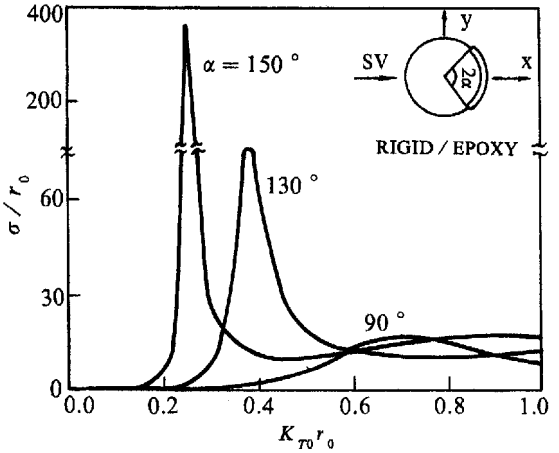


Fig. 9. The SCS vs $K_{T0}r_0$ for SV-wave incidence in $x$-direction ($\theta_0 = 0°$) with $\alpha = 150°$, 130°, and 90°.

inclusion experiences a low-frequency resonance which becomes stronger as $\alpha$ is increased, just like the DSIF and SCS. A noteworthy phenomenon is that the resonances for the translation in $y$-direction and rotation are more pronounced and occur at a lower frequency than those for the translation in $x$-direction. This is why the DSIF and SCS for P-wave

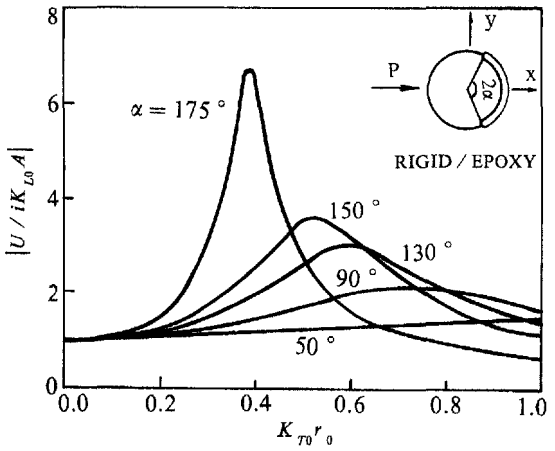


Fig. 10. The motion of the inclusion for P-wave incidence in $x$-direction ($\theta_0 = 0°$) with $\alpha = 175°$, 150°, 130°, 90°, and 50°: RBT in $x$-direction.

incidence in $y$-direction and SV-wave in $x$-direction exhibit a stronger low-frequency resonance than those for P-wave in $x$-direction. An explanation of the mechanism of this behavior of the low-frequency resonance is imperatively desired.

Finally, the effects of the mass density ratio $\rho_1/\rho_0$ and Poisson ratio $\nu_0$ on the SCS is displayed in Figs 13 and 14, respectively. As $\rho_1/\rho_0$ is increased and/or $\nu_0$ is decreased, the low-frequency resonance becomes stronger.

## 10. CONCLUDING REMARKS

The singular integral equation technique is used in this series of papers to solve the problems of elastic wave scattering from a partially debonded inclusion. The method allows for multiple debonds and is proved to be very efficient, especially in dealing with the in-plane strain problem involving the oscillatory behavior of stresses near the crack tips. Numerical results are presented for various cases and the asymptotic explicit expressions in the quasi-static limit and the small debond limit are obtained. They are in good agreement with those of others [e.g. Yang and Norris (1991, 1992), Coussy (1983), Toya (1974), etc.]. Although the analysis is limited to the case of a rigid inclusion, it can be easily extended to the elastic case by considering the wave fields in the inclusion. Furthermore, the present method may also be applied to the case of an elliptic inclusion. Indeed we have used a similar approach to solve the dynamic problem of an elliptic arc crack which may be viewed as a special case of an interface crack (Wang and Wang, 1994).

As in the paper by Yang and Norris (1992), the debonds in the present paper are also modeled as interface cracks of which the faces are assumed not to contact each other. This assumption results in the oscillatory form of the stress singularity which is impossible in practical cases. Comninou (1977) presented a new model for a flat interface crack to suppress this unrealistic singularity by allowing closure of the crack tips. If closure takes place at the crack tips, the stress singularity has an entirely different character. Zhou *et al.* (1987) has applied Comninou's model to the dynamic case of a flat interface crack and demonstrated the dependence of the closure region on the frequency. Their model and method can certainly be used to arc-shaped interface cracks considered in this paper. However, the analysis is so complicated that it must be reported in a paper longer that the present one. Therefore, we have to leave it for future study.

Even if we considered the closure of the crack tips, we are still far away from the practical case. In fact, closure may take place, not only at the crack tips, but also anywhere on the crack faces and friction may also exist in the closure region. Closure or contact of the crack faces has significant influence on the low-frequency resonance. Generally, it will make the resonance not so strong as we have demonstrated in present paper. Indeed, the analysis involving such closure or contact is of more practical importance. However, the

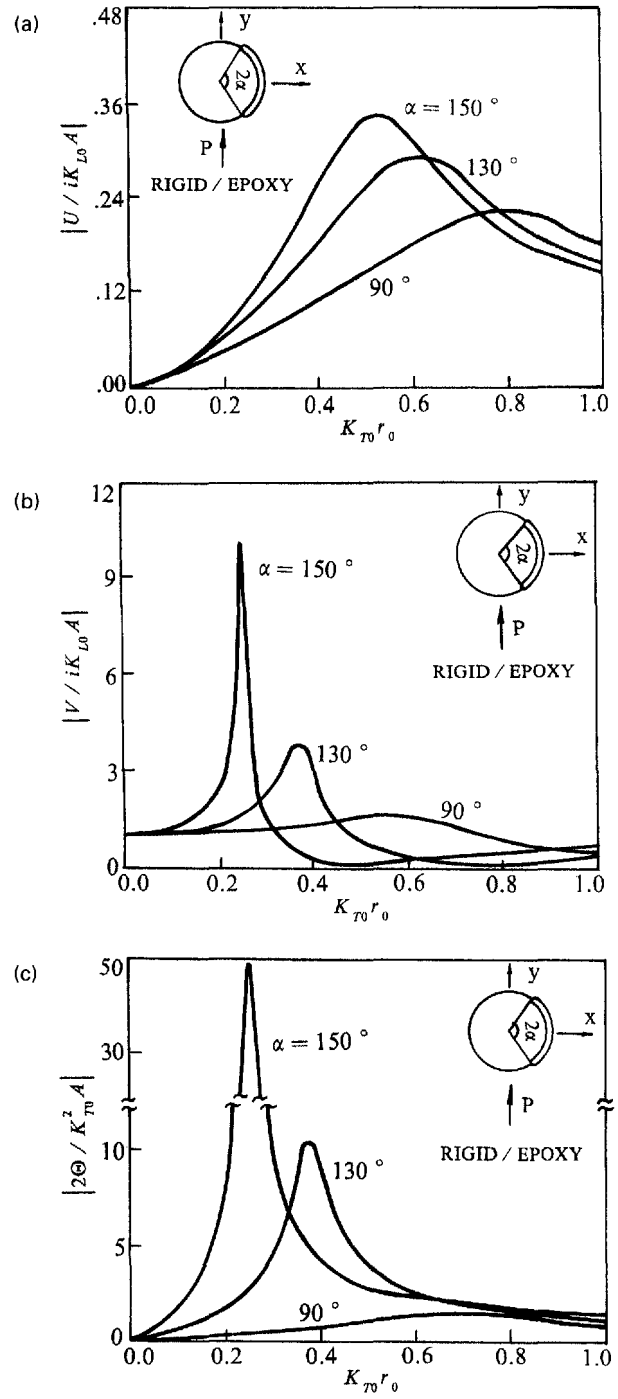


Fig. 11. The motion of the inclusion for P-wave incidence in $y$-direction ($\theta_0 = 90°$) with $\alpha = 150°$, 130°, and 90°. (a) RBT in $x$-direction. (b) RBT in $y$-direction. (c) RBR around $z$-axis.

extent of the closure region and even where the closure takes place will remain in open conditions of the problem. This will make the problem almost intractable. Therefore, the closure is ignored in the present analysis for simplicity, which means that the results are valid only in the situations where the crack is prestressed to remain opening. Such an assumption has been made in most published works concerning the dynamic problem of cracks, including the references cited in this paper. In fact, any analytical method is ineffective if the dynamic contact of the crack faces is taken into account. A computational scheme, such as finite element method (FEM) or boundary element method (BEM), may be a powerful tool in dealing with such a problem. For instance, Hirose (1994) has solved

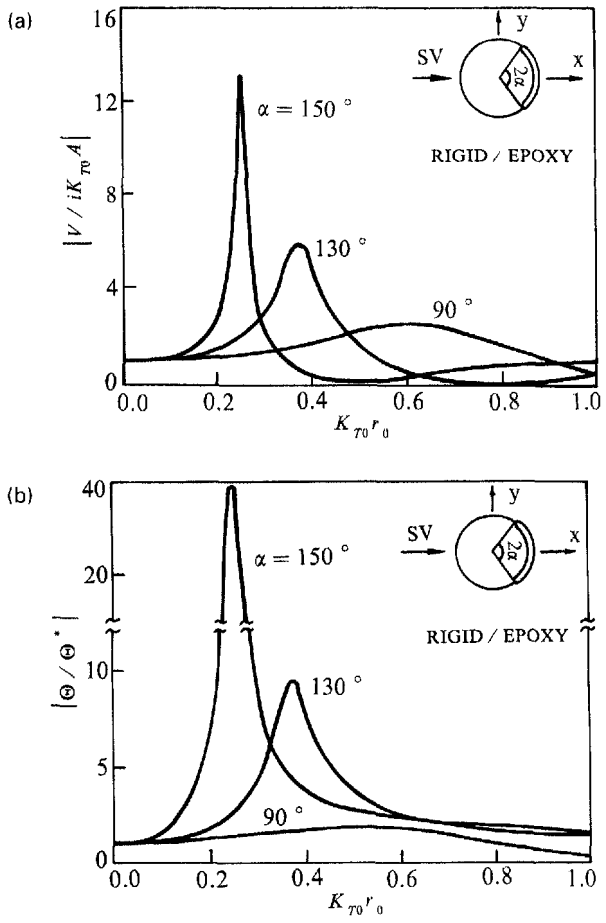


Fig. 12. The motion of the inclusion for SV-wave incidence in $x$-direction ($\theta_0 = 0°$) with $\alpha = 150°$, 130°, and 90°: (a) RBT in $y$-direction, and (b) RBR around $z$-axis.

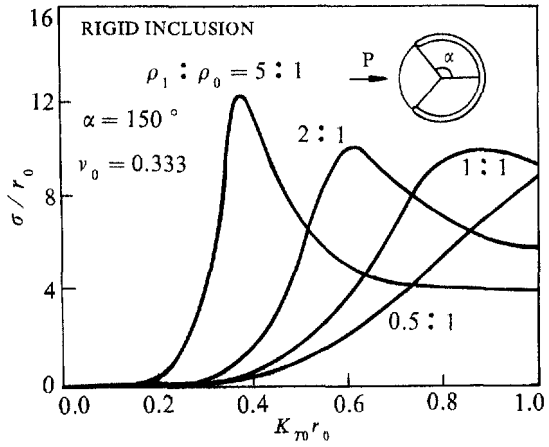


Fig. 13. The SCS vs $K_{T0}r_0$ for different values of $\rho_1/\rho_0$ with $\nu_0 = 0.333$, $\alpha = 150°$ and $\theta_0 = 0°$, P-wave incidence.

the scattering problem of a crack with contact-boundary conditions by BEM, while Liu *et al.* (1994) have considered the similar problem by FEM. One may expect that the dynamic problem of arc-shaped interface cracks with contact faces will be solved by FEM or BEM, instead of an analytical method, in the near future.

Although the present results are somewhat limited, they are expected to have applications to fields such as earthquake engineering, nondestructive evaluation of materials,

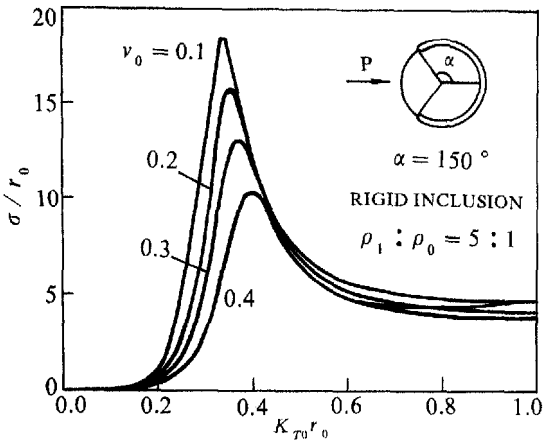


Fig. 14. The SCS vs $K_{T0}r_0$ for different values of $\nu_0$ with $\rho_1/\rho_0 = 5$, $\alpha = 150°$ and $\theta_0 = 0°$, P-wave incidence.

the forecast of dynamic failure of composite materials and structures, etc. Norris and Yang (1991) and Coussy (1986) have demonstrated some applications of their solutions. We will discuss in details the possible applications of the present results afterwards.

*Acknowledgement*—We are grateful to the reviewers for helpful comments.

## REFERENCES

Abramowitz, M. and Stegun, I. A. (1965). *Handbook of Mathematical Functions*. Dover, New York.
Comninou, M. (1977). The interface crack. *J. Appl. Mech.* **44,** 631–636.
Coussy, O. (1983). Scattering of elastic waves by an inclusion with an interface crack. *Wave Motion* **6,** 223–236.
Coussy, O. (1986). The influence of interface cracks on wave motion in fiber reinforced elastic solids. *J. Mecanique Theor. Appl.* **5,** 803–823.
Dundurs, J. (1969). Discussion of a paper by Bogy, D. B. *J. Appl. Mech.* **36,** 650–652.
Erdogan, F. and Gupta, G. D. (1971). Layered composites with an interface flaw. *Int. J. Solids Structures* **7,** 1089–1107.
Hirose, S. (1994). 2-D scattering by a crack with contact-boundary conditions. *Wave Motion* **19,** 37–49.
Liu, J. B., Wang, D. and Yao, L. (1994). Contact force model for the dynamic response of cracks. *Comput. Structures* **52,** 659–666.
Muskhelishvili, N. I. (1953). *Singular Integral Equations*. Noordhoff, Leyden.
Norris, A. and Yang, Y. (1991). Static and dynamic axial loading of a partially bonded fiber. *Mech. Mater.* **11,** 163–175.
Pao, Y. H. and Mow, C. C. (1973). *Diffraction of Elastic Waves and Dynamic Stress Concentrations*. Crane and Russak, New York.
Srivastava, K. N. Gupta, O. P. and Palaiya, R. M. (1978). Interaction of elastic waves in two bonded dissimilar elastic half-planes having Griffith crack at interface. *Int. Int. J. Fract.* **14,** 145–154.
Toya, M. (1974). A crack along the interface of a circular inclusion embedded in an infinite solid. *J. Mech. Phys. Solids* **22,** 325–348.
Wang, Y. S. and Wang, D. (1994). Elliptic arc crack subjected to anti-plane shear wave. *Engng Fract. Mech.* **48,** 289–297.
Wang, Y.-S. and Wang, D. (1996). Scattering of elastic waves by a rigid cylindrical inclusion partially debonded from its surrounding matrix—I. SH case. *Int. J. Solids Struct.* **33,** 2789–2815.
Yang, H. J. and Bogy, D. B. (1985). Elastic wave scattering from an interface crack in a layered half-space. *J. Appl. Mech.* **52,** 42–50.
Yang, Y. and Norris A. N. (1991). Shear wave scattering from a debonded fiber. *J. Mech. Phys. Solids* **39,** 273–294.
Yang, Y. and Norris, A. (1992). Longitudinal wave scattering from a partially bonded fiber. *Wave Motion* **15,** 43–59.
Zhou, Z. Z., Wang, X. D. and Wang, D. (1987). The dynamic behavior near a crack with closed tip on the interface of two bonded dissimilar elastic half planes. In *Proc. Int. Conf. on Fracture and Fracture Mechanics* (Edited by C. Ouyang), pp. 165–169. Fudan University Press, Shanghai.

## APPENDIX

$$N_m^{(11)} = \begin{cases} r_0^{-1}[D_m^{-1}K_{T0}^3 r_0^3 H_m^{(1)}(K_{L0}r_0)H_m^{(1)\prime}(K_{T0}r_0) - 2], m \neq \pm 1 \\ r_0^{-1}\{D_1^{-1}[K_{T0}^3 r_0^3 H_m^{(1)}(K_{L0}r_0)H_m^{(1)\prime}(K_{T0}r_0) - \rho K_{T0}^2 r_0^2 H_m^{(1)}(K_{L0}r_0)H_m^{(1)\prime}(K_{T0}r_0)] - 2\}, \quad m = \pm 1 \end{cases} \tag{A1}$$

$$N_m^{(12)} = -N_m^{(21)} = \begin{cases} imr_0^{-1}[2 - D_m^{-1} K_{T0}^2 r_0^2 H_m^{(1)}(K_{L0}r_0) H_m^{(1)}(K_{T0}r_0)], m \neq \pm 1 \\ imr_0^{-1}[2 - D_1^{-1}(1-\rho) K_{T0}^2 r_0^2 H_m^{(1)}(K_{L0}r_0) H_m^{(1)}(K_{T0}r_0)], m = \pm 1 \end{cases} \tag{A2}$$

$$N_m^{(22)} = \begin{cases} r_0^{-1}[D_m^{-1} K_{L0} K_{T0}^2 r_0^3 H_m^{(1)\prime}(K_{L0}r_0) H_m^{(1)}(K_{T0}r_0) - 2], m \neq 0, \pm 1 \\ -r_0^{-1} \dfrac{K_{T0}^2 r_0^2 [K_{T0}r_0 H_0^{(1)}(K_{T0}r_0) + 2H_0^{(1)\prime}(K_{T0}r_0)]}{K_{T0}^2 r_0^2 H_0^{(1)\prime}(K_{T0}r_0) - 4\rho[K_{T0}r_0 H_0^{(1)}(K_{T0}r_0) + 2H_0^{(1)\prime}(K_{T0}r_0)]}, m = 0 \\ r_0^{-1}\{D_1^{-1}[K_{L0} K_{T0}^2 r_0^3 H_m^{(1)\prime}(K_{T0}r_0) - \rho K_{T0}^2 r_0^2 H_m^{(1)}(K_{L0}r_0) H_m^{(1)}(K_{T0}r_0)] - 2\}, m = \pm 1 \end{cases} \tag{A3}$$

For $D_m$ ($m \neq \pm 1$) and $D_1$ in eqns (A1), (A2), and (A3), see eqns (21) and (23):

$$C_{kj}^{(11)} = c_1 \int_{-1}^{1} \int_{-1}^{1} W_f(\eta) P_f^{(\alpha_1,\beta_1)}(\eta) Q_{11}(\eta, \xi)\, d\eta\, W_f^{-1}(\xi) P_k^{(-\alpha_1,-\beta_1)}(\xi)\, d\xi \tag{A4}$$

$$C_{kj}^{(12)} = c_1 \int_{-1}^{1} \int_{-1}^{1} W_g(\eta) P_j^{(\beta_1,\alpha_1)}(\eta) Q_{12}(\eta, \xi)\, d\eta\, W_f^{-1}(\xi) P_k^{(-\alpha_1,-\beta_1)}(\xi)\, d\xi \tag{A5}$$

$$C_{kj}^{(21)} = c_1 \int_{-1}^{1} \int_{-1}^{1} W_f(\eta) P_j^{(\alpha_1,\beta_1)}(\eta) Q_{21}(\eta, \xi)\, d\eta\, W_g^{-1}(\xi) P_k^{(-\beta_1,-\alpha_1)}(\xi)\, d\xi \tag{A6}$$

$$C_{kj}^{(22)} = c_1 \int_{-1}^{1} \int_{-1}^{1} W_g(\eta) P_j^{(\beta_1,\alpha_1)}(\eta) Q_{22}(\eta, \xi)\, d\eta\, W_g^{-1}(\xi) P_k^{(-\beta_1,-\alpha_1)}(\xi)\, d\xi \tag{A7}$$

$$F_k = \int_{-1}^{1} \bar{\sigma}(\xi) W_f^{-1}(\xi) P_k^{(-\alpha_1,-\beta_1)}(\xi)\, d\xi \tag{A8}$$

$$G_k = \int_{-1}^{1} \bar{\tau}(\xi) W_g^{-1}(\xi) P_k^{(-\beta_1,-\alpha_1)}(\xi)\, d\xi. \tag{A9}$$